AD-A070 482 MARYLAND UNIV COLLEGE PARK DEPT OF PHYSICS AND ASTRONOMY F/G 20/3
INTENSE MICROWAVE GENERATION BY THE NEGATIVE-MASS INSTABILITY,(U)
1978 H UHM, R C DAVIDSON N00014-75-C-0309

UNCLASSIFIED PUB-78-029 NL

| OF |
AD
A070482

END
DATE
FILMED
8-79
DDC

Code 6702

PREPRINT #708P002

INTENSE MICROWAVE GENERATION BY THE NEGATIVE-MASS INSTABILITY

Hwan-sup Uhm
Department of Physics and Astronomy
University of Maryland, College Park, Md. 20742

and

Ronald C. Davidson*
Division of Magnetic Fusion Energy
Energy Research and Development Administration
Washington, D. C. 20545

Physics Publication Number 78-029

1978

Work on this report was supported by ONR Contract N00014-75-C-0309 and/or N00014-67-A-0239 monitored by NRL Code 6702.

UNIVERSITY OF MARYLAND
DEPARTMENT OF PHYSICS AND ASTRONOMY
COLLEGE PARK, MARYLAND

AD A070482

DDC ACCESSION NUMBER

II

LEVEL

DDC PROCESSING DATA

PHOTOGRAPH

THIS SHEET

RETURN TO DDA-2 FOR FILE

1

INVENTORY

Preprint 708P002, Physics Pub. 78-029

DOCUMENT IDENTIFICATION

DISTRIBUTION STATEMENT A

Approved for public release;
Distribution Unlimited

DISTRIBUTION STATEMENT

Accession For	
NTIS GRA&I	X
DDC TAB	
Unannounced	
Justification	
By	
Distribution/	
Availability Codes	
Dist.	Avail and/or special
A	

DISTRIBUTION STAMP

DDC
RECEIVED
JUN 28 1979
D

DATE ACCESSIONED

79 06 27 301

DATE RECEIVED IN DDC

PHOTOGRAPH THIS SHEET

RETURN TO DDA-2

Work on this report was supported
by ONR Contract N00014-75-C-0309
and/or N00014-67-A-0239
monitored by NRL Code 6702.

INTENSE MICROWAVE GENERATION BY THE NEGATIVE-MASS INSTABILITY

Hwan-sup Uhm
Department of Physics and Astronomy
University of Maryland, College Park, Md. 20742

and

Ronald C. Davidson*
Division of Magnetic Fusion Energy
Energy Research and Development Administration
Washington, D. C. 20545

This paper examines the negative-mass stability properties of an E-layer for transverse electric (TE) and transverse magnetic (TM) waveguide modes in a conducting cylinder. The analysis is carried out for a relativistic nonneutral E-layer aligned parallel to a uniform axial magnetic field $B_0\hat{e}_z$, within the context of the assumptions that the electron motion is ultrarelativistic (γ_0>>1) and that $(\nu/\gamma_0)^{1/3}$<<1, where ν is Budker's parameter and $\gamma_0 mc^2$ is the electron energy. One of the most important features of the analysis is that the axial energy spread can have a large influence of stability behavior for both the TE and TM waveguide modes. By appropriate choice of system parameters, it is shown that the spectrum of microwave radiation generated by the negative-mass instability can be very narrow-band.

* On leave of absence from the University of Maryland, College Park, Md.

I. INTRODUCTION

The major recent experimental interest in relativistic electron beams originates from several diverse research areas. These include: research on plasma confinement schemes such as Astron[1], high-power microwave generation[2-6], and electron ring accelerators[7-9]. One of the most basic instabilities that characterizes a relativistic E-layer is the negative-mass instability[10-13]. The azimuthal bunching of the beam electrons associated with this instability may provide the mechanism for intense microwave generation recently observed in several experiments[6-9]. In this regard, the resonant interaction of transverse electric (TE) or transverse magnetic (TM) waveguide modes (inside a conducting cylinder) with beam-cyclotron modes has also been studied as a mechanism for intense microwave generation[14]. Moreover, the influence of an energy spread on the negative-mass instability has been investigated in the literature[9-12]. The present paper examines the negative-mass stability properties of an intense relativistic E-layer for both the TE and TM waveguide modes, making use of the dispersion relation already developed in Ref. 12. One of the most important features of the analysis is that the axial energy spread can have a large influence on stability behavior. By appropriate choice of system parameters, it is also shown that the spectrum of microwave radiation generated by the negative-mass instability can be very narrow-band.

The present analysis is carried out for an infinitely long E-layer aligned parallel to a uniform magnetic field $B_0\hat{e}_z$ (Fig. 1), assuming that the azimuthal electron motion is ultrarelativistic ($\gamma_0 >> 1$) and that

$(\nu/\gamma_0)^{1/3} \ll 1$, where $\nu = N_e e^2/mc^2$ is Budker's parameter, N_e is the number of electrons per unit axial length of the E-layer, and $\gamma_0 mc^2$ is the characteristic electron energy. A brief description of the theoretical model and equilibrium configuration is given in Sec. II. For an ultra-relativistic, infinitesimally thin E-layer, the dispersion relation[12] for the negative-mass instability simplifies considerably [Eq. (3)].

A detailed analytic investigation of the negative-mass instability for TE and TM waveguide modes is carried out in Sec. III. Introducing the dimensionless parameter [Eq. (12)]

$$\Delta = (\Delta E/\gamma_0 mc^2)\,(\gamma_0/\nu)^{2/3} \quad ,$$

which is a measure of the characteristic relative strength of the axial energy spread (ΔE) and the number of electrons per unit axial length ($\nu = N_e e^2/mc^2$), we find that [Eqs. (17) and (22)]

$$g_{\ell n}^{E^2} > \ell^2[2\Delta(\ell^2 - \alpha_{\ell n}^2 R_0^2/R_c^2)/3]^3 \quad , \quad \text{TE mode,}$$

$$g_{\ell n}^{M^2} > \ell^2[2\Delta(\ell^2 - \beta_{\ell n}^2 R_0^2/R_c^2)/3]^3 \quad , \quad \text{TM mode,}$$

are necessary and sufficient conditions for instability. Here $g_{\ell n}^E$ and $g_{\ell n}^M$ are the geometric factors [Eqs. (9) and (11)] for the TE and TM modes, ℓ is the azimuthal harmonic number, R_0 and R_c are the radii of the E-layer and the conducting wall, and $\beta_{\ell n}$ and $\alpha_{\ell n}$ are zeros of the Bessel function, $J_\ell(y)$, and its first derivative, $J_\ell'(y)$, respectively. Evidently the axial energy spread (Δ) has a very important influence on stability behavior (Secs. III and IV). A detailed numerical analysis of the dispersion relation is presented in Sec. IV, where stability properties are investigated for a broad range of system parameters.

Finally, we note that the stability criterion in Eq. (17) can be used to control the frequency of the microwave radiation generated by the azimuthal electron bunching associated with the negative-mass instability. Since the stabilization produced by the axial energy spread (Δ) is effective only for perturbations with sufficiently large axial wavenumber[12] ($k^2R_0^2=\ell^2-\alpha_{\ell n}^2R_0^2/R_c^2 \gtrsim 1$), we conclude that selecting the value of R_0/R_c very close to $\ell/\alpha_{\ell n}$ and introducing a modest amount of axial energy spread ($\Delta \gtrsim 1$) can stabilize all modes except those with real frequency $\omega_r \simeq \ell\omega_c \simeq [\alpha_{\ell n}R_0/R_c]\omega_c$. The present analysis also shows that the preferential excitation of a single unstable mode is more straightforward for TE than for TM modes (Secs. III and IV).

II. THEORETICAL MODEL AND EQUILIBRIUM CONFIGURATION

As illustrated in Fig. 1, the equilibrium configuration consists of a relativistic nonneutral E-layer that is infinite in axial extent and aligned parallel to a uniform applied magnetic field $B_0\hat{e}_z$. The radii of the E-layer and the cylindrical conducting wall are denoted by R_0 and R_c, respectively. The mean motion of the E-layer is in the azimuthal direction with average velocity $V_\theta^0\hat{e}_\theta$, which produces an axial self-magnetic field $B_{0z}^s\hat{e}_z$. The applied magnetic field provides radial confinement of the electrons. As shown in Fig. 1, we introduce a cylindrical polar coordinate system (r, θ, z) with the z-axis coinciding with the axis of symmetry; r is the radial distance from the z-axis, and θ is the polar angle in a plane perpendicular to the z-axis.

The following are the main assumptions pertaining to the present analysis:

(a) The E-layer is infinitesimally thin ($a/R_0 \to 0$, where a is the half-thickness of E-layer) and completely unneutralized (f=0, where f is the fractional charge neutralization).

(b) The electron motion is ultrarelativistic ($\gamma_0 \gg 1$), and the mean equilibrium motion of the E-layer is in the azimuthal direction ($V_z^0=0$, where V_z^0 is the mean axial velocity of an electron fluid element).

(c) It is further assumed that

$$(\nu/\gamma_0)^{1/3} \ll 1 \quad , \tag{1}$$

where $\nu = N_e e^2/mc^2$ is Budker's parameter, N_e is the number of electrons per unit axial length of the E-layer, c is the speed of light in vacuo, $\gamma_0 mc^2$ is the characteristic energy of an electron in the E-layer, and -e and m are the charge and rest mass, respectively, of the electron.

The inequality in Eq. (1) indicates that the E-layer is very tenuous.

The equilibrium and negative-mass stability properties have been investigated in Ref. 12 for the choice of electron distribution function in which all electrons have the same value of canonical angular momentum and a step-function distribution in axial momentum p_z. The resulting dispersion relation for the negative-mass instability is given by[12]

$$(\omega-\ell\omega_c)^2 = -\frac{c^2}{R_0^2}\left[\frac{\nu}{\gamma_0}\,\frac{g\omega_c}{\omega}\,(\mu\ell^2-k^2R_0^2)-2k^2R_0^2\,\frac{\Delta E}{\gamma_0 mc^2}\right] , \tag{2}$$

where ω is the complex eigenfrequency, $\omega_c=eB_0/\gamma_0 mc$ is the electron cyclotron frequency, ℓ is the azimuthal harmonic number, k is the axial wavenumber, ΔE is the axial energy spread, and the factors g and μ are defined in Eqs. (44) and (51) of Ref. 12. [For a detailed derivation of Eq. (2), see Ref. 12.]

Making use of Assumptions (a) - (c) [which imply that $V_\theta^0/c = (\gamma_0^2-1)^{1/2}/\gamma_0 \simeq 1$ and $\mu\simeq 1$), and approximating $\omega\simeq\ell\omega_c$, Eq. (2) can be further simplified to give

$$(\omega-\ell\omega_c)^2 = -\frac{2c^2}{R_0^2}\left[\frac{\nu}{\gamma_0}\,\frac{G(p)}{\ell} - \kappa^2R_0^2\,\frac{\Delta E}{\gamma_0 mc^2}\right] , \tag{3}$$

where the geometric factor G(p) is defined by

$$G(p) = \ell^2/(b_-+b_+) - k^2R_0^2/(d_-+d_+), \tag{4}$$

with

$$p = (\omega^2/c^2 - k^2)^{1/2} . \tag{5}$$

In Eq. (4), the sums of the wave admittances[12] are defined by

$$b_- + b_+ = - \frac{2\ell J'_\ell(pR_c)/\pi p^2 R_0^2}{J'_\ell(pR_0)[J'_\ell(pR_0)N'_\ell(pR_c) - J'_\ell(pR_c)N'_\ell(pR_0)]} ,$$

$$d_- + d_+ = \frac{2J_\ell(pR_c)/\ell\pi}{J_\ell(pR_0)[J_\ell(pR_0)N_\ell(pR_c) - J_\ell(pR_c)N_\ell(pR_0)]} , \tag{6}$$

where the prime (') denotes (1/p)(d/dr), and $J_\ell(y)$ and $N_\ell(y)$ are Bessel functions of the first and second kind, respectively. The resonant interaction of the negative-mass instability with the normal modes of the grounded conducting cylinder (radius = R_c) is investigated in Sec. III. The analysis makes use of the vacuum transverse electric (TE) and transverse magnetic (TM) waveguide modes, which form a convenient basis to express a general electromagnetic field configuration within a cylindrical waveguide.

III. EXCITATION OF ELECTROMAGNETIC WAVEGUIDE MODES

In this section, we investigate the negative-mass stability properties for the TE and TM waveguide modes. In the absence of the E-layer, the vacuum dispersion relation for the waveguide modes is given by

$$(\omega^2/c^2 - k^2)\, R_c^2 = \begin{cases} \alpha_{\ell n}^2 , & \text{TE mode,} \\ \beta_{\ell n}^2 , & \text{TM mode,} \end{cases} \tag{7}$$

where $\alpha_{\ell n}$ and $\beta_{\ell n}$ are the nth roots of $J_\ell'(\alpha_{\ell n}) = 0$ and $J_\ell(\beta_{\ell n}) = 0$, respectively. Taylor expanding Eq. (6) about $\omega=\ell\omega_c$, it is straightforward to show for the TE mode that sum of the magnetic wave admittances $(b_-+b_+)_{TE}$ can be expressed as

$$(b_-+b_+)_{TE} = -\,(\,\ell^2/\,g_{\ell n}^E)\,(\omega-\ell\omega_c)/\omega_c \quad , \tag{8}$$

where the geometric factor $g_{\ell n}^E$ is defined by

$$g_{\ell n}^E(R_0/R_c) = R_0^4\alpha_{\ell n}^2[J_\ell'(\alpha_{\ell n}R_0/R_c)]^2/[R_c^4 J_\ell''(\alpha_{\ell n})J_\ell(\alpha_{\ell n})]\ . \tag{9}$$

In obtaining Eq. (9), use has been made of Wronskian, $J_\ell(y)N_\ell'(y)-J_\ell'(y)N_\ell(y)=(2/\pi y)$, and $J_\ell'(\alpha_{\ell n})=0$. Similarly, for the TM mode, the sum of the electric wave admittances $(d_-+d_+)_{TM}$ can be expressed as

$$(d_-+d_+)_{TM} = -[(\ell^2 - \beta_{\ell n}^2 R_0^2/R_c^2)/\,g_{\ell n}^M]\,(\omega-\ell\omega_c)/\omega_c \quad , \tag{10}$$

where the geometric factor $g_{\ell n}^M$ is defined by

$$g_{\ell n}^M(R_0/R_c) \;=\; R_0^2(\ell^2-\beta_{\ell n}^2R_0^2/R_c^2)[J_\ell(\beta_{\ell n}R_0/R_c)]^2/[R_cJ_\ell'(\beta_{\ell n})]^2. \tag{11}$$

For the TE mode, the contribution of (d_-+d_+) to the geometric factor G(p) in Eq. (4) has been neglected in comparison with the contribution from $(b_-+b_+)_{TE}$, since $|\omega-\ell\omega_c|/\omega_c \approx (\nu/\gamma_0)^{1/3} << 1$. On the

other hand, the main contribution to the geometric factor G(p) for the TM mode is determined by $(d_-+d_+)_{TM}$. For convenience in the subsequent analysis, we define the normalized energy spread

$$\Delta = (\Delta E/\gamma_0 mc^2)(\gamma_0/\nu)^{2/3} \tag{12}$$

and introduce the frequency

$$\omega_g = \omega_c(\nu/\gamma_0)^{1/3} \quad . \tag{13}$$

A. TE Mode Dispersion Relation

Substituting Eqs. (4) and (8) into Eq. (3) and making use of the definitions in Eqs. (12) and (13), we obtain the approximate dispersion relation,

$$x^3 - 2\Delta(\ell^2 - \alpha_{\ell n}^2 R_0^2/R_c^2)\, x - 2g_{\ell n}^E/\ell = 0 \quad , \tag{14}$$

for the TE mode. In Eq. (14), the normalized eigenfrequency x is defined by

$$x = (\omega - \ell\omega_c)/\omega_g \quad . \tag{15}$$

Defining $\omega=\omega_r+i\omega_i$, it follows from Eq. (15) that the real frequency ω_r can be approximated by $\omega_r=\ell\omega_c$, since $|\omega-\ell\omega_c|/\omega_c \lesssim \omega_g/\omega_c << 1$. The discriminant D_E^2 for the third-order polynominal in Eq. (14) is given by

$$D_E^2 = (g_{\ell n}^E/\ell)^2 - [2\Delta(\ell^2 - \alpha_{\ell n}^2 R_0^2/R_c^2)/3]^3 \quad . \tag{16}$$

Therefore, the necessary and sufficient condition for the negative-mass instability (TE mode) can be expressed as $D_E^2>0$, or equivalently,

$$g_{\ell n}^{E^2} > \ell^2 [2\Delta(\ell^2 - \alpha_{\ell n}^2 R_0^2/R_c^2)/3]^3 \quad . \tag{17}$$

Moreover, the growth rate ω_i for the unstable branch can be expressed as

$$\omega_i = (3/4)^{1/2}|(|g^E_{\ell n}|/\ell + D_E)^{1/3} - (|g^E_{\ell n}|/\ell - D_E)^{1/3}|\omega_g \qquad (18)$$

for the TE mode.

As a check on the growth rate given in Eq. (18), it is instructive to consider the E-layer with negligibly small axial energy spread (Δ=0). In this case, Eq. (18) can be expressed as

$$\omega_i = (3/4)^{1/2} (2|g^E_{\ell n}|/\ell)^{1/3} \omega_g$$

which is identical to the result obtained by Sprangle[14] within the framework of the macroscopic sheet model (assuming V^0_z=0 and considering the TE-synchronous mode).

It is evident from Eq. (17) that perturbations with sufficiently large axial wavenumber $[kR_o=(\ell^2-\alpha^2_{\ell n}R^2_0/R^2_c)^{1/2}\gtrsim 1]$ can be effectively stabilized by the axial energy spread[12]. In this context, it is possible to stabilize all of the harmonic perturbations by a modest axial energy spread ($\Delta\gtrsim 1$), except for one select perturbation corresponding to $\ell\simeq\alpha_{\ell n}R_0/R_c$. Evidently, by appropriate choice of beam radius (R_0/R_c) and the axial energy spread (Δ), a narrow spectrum of microwave radiation can be produced by the negative-mass instability. However, a small but nonzero axial wavenumber is necessary for this particular perturbation ($\ell\simeq\alpha_{\ell n}R_0/R_c$), in order for the radiation energy to propagate axially out of the system. From Eqs. (9), (16) and (18), and the relation $R_0/R_c=\ell/\alpha_{\ell n}$, the corresponding maximum growth rate can be expressed as

$$\omega_i = (3/4)^{1/2}\{2\ell^3[J'_\ell(\ell)]^2/\alpha^2_{\ell n}J''_\ell(\alpha_{\ell n})J_\ell(\alpha_{\ell n})\}^{1/3} \qquad (19)$$

for the TE mode.

B. TM Mode Dispersion Relation

Substituting Eqs. (4) and (10) into Eq. (3) gives the dispersion relation

$$x^3 - 2\Delta(\ell^2 - \beta_{\ell n}^2 R_0^2/R_c^2)\, x - 2g_{\ell n}^M/\ell = 0 \qquad (20)$$

for the TM mode. In obtaining Eq. (20), use has been made of Eqs. (12), (13) and (15). The discriminant D_M^2 for Eq. (20) is given by

$$D_M^2 = (g_{\ell n}^M/\ell)^2 - [2\Delta(\ell^2 - \beta_{\ell n}^2 R_0^2/R_c^2)/3]^3 \qquad (21)$$

and the necessary and sufficient condition for instability can be expressed as

$$g_{\ell n}^{M^2} > \ell^2 [2\Delta(\ell^2 - \beta_{\ell n}^2 R_0^2/R_c^2)/3]^3 \quad . \qquad (22)$$

From Eq. (20), the growth rate ω_i for the unstable branch (TM mode) is given by

$$\omega_i = (3/4)^{1/2} \left| (|g_{\ell n}^M|/\ell + D_M)^{1/3} - (|g_{\ell n}^M|/\ell - D_M)^{1/3} \right| \omega_g \qquad (23)$$

Unlike the TE mode, it is not possible to make one select TM mode unstable, since $g_{\ell n}^M = 0$ when $kR_0 = (\ell^2 - \beta_{\ell n}^2 R_0^2/R_c^2)^{1/2} = 0$ [see also the discussion following Eq. (18)].

We conclude this section by noting that the present analysis can be generalized to the case of an intense E-layer with finite thickness, although the corresponding analytic treatment is more complicated.

IV. STABILITY ANALYSIS

The growth rate ω_i=Imω has been calculated numerically from Eqs. (18) and (23) for a broad range of the parameters R_0/R_c, ℓ, n, kR_0, and $\Delta=(\Delta E/\gamma_0 mc^2)(\gamma_0/\nu)^{2/3}$. In this section, we summarize the essential features of these stability studies. The growth rate is measured in units of the frequency $\omega_g=\omega_c(\nu/\gamma_0)^{1/3}$.

Figure 2 shows a plot of the normalized growth rate ω_i/ω_g versus R_0/R_c obtained from (a) Eq. (14) (TE mode) and (b) Eq. (20) (TM mode), for Δ=0, n=1 and several values of ℓ. Several points are noteworthy in Fig. 2. First, the maximum growth rate and the range of R_0/R_c corresponding to instability increase rapdily as the harmonic number ℓ is increased. This feature is also evident from Eq. (19) for the TE mode. Second, the maximum growth rate for the TE mode occurs when $R_0/R_c=\ell/\alpha_{\ell n}$, whereas the growth rate for the TM mode vanishes abruptly at the cut-off value $R_0/R_c=\ell/\beta_{\ell n}$ (see also Sec. III). Third, the range of R_0/R_c corresponding to instability approaches unity as the harmonic number ℓ is increased. For example, the $(\ell,n)=(1,1)$ TM mode is unstable over the range $0<R_0/R_c<0.25$, whereas the $(\ell,n)=(15,1)$ TM mode is unstable over the range $0.3\leq R_0/R_c<0.8$ [see Fig. 2(b)]. Fourth, for the same values of (ℓ,n), the TE mode is more unstable than the TM mode. For example, for $(\ell,n)=(9,1)$, the maximum growth rate of the TE mode is $\omega_i \simeq 1.3\ \omega_g$, whereas the maximum growth rate is $\omega_i \simeq 0.76\ \omega_g$ for the TM mode (see Fig. 2).

Shown in Fig. 3 are plots of the normalized growth rate ω_i/ω_g versus R_0/R_c obtained from (a) Eq. (14) (TE mode), and (b) Eq. (20) (TM mode), for Δ=0, ℓ=8 and several values of n. The maximum growth rate in Figs. 3(a) and 3(b) is reduced by increasing the value of n. Since $\alpha_{\ell n}$ is an increasing function of n, this feature is also evident from Eq. (19) (TE mode). Finally, we note from Fig. 3 that the range of R_0/R_c

corresponding to instability decreases to zero as the mode number n is increased.

An example is now investigated to illustrate the influence of axial energy spread (Δ) on stability behavior. Figure 4 shows a plot of the normalized growth rate ω_i/ω_g versus Δ for ℓ=6, n=1, and normalized axial wavenumber kR_0=2. The growth rates are obtained from Eq. (14) (TE mode) and Eq. (20) (TM mode). To maintain the same value of kR_0(=2) for both modes, we choose R_0/R_c=0.754 for the TE mode and R_0/R_c=0.569 for the TM mode. As shown in Fig. 4, Δ = 0.13 is sufficient energy spread to stabilize the TM mode, whereas Δ=0.35 is required for stabilization of the TE mode. We conclude that an axial energy spread is an effective means for stabilizing perturbations with sufficiently short axial wavelength ($k \gtrsim 1/R_0$, say).[12] Moreover, a smaller energy spread is required to stabilize the TM mode than the TE mode (Fig. 4).

Of considerable interest for experimental applications is the stability behavior for specified (ℓ,n) and several values of Δ. Typical results are shown in Figs. 5 and 6 where ω_i/ω_g is plotted versus R_0/R_c for ℓ=2 (Fig. 5) and ℓ=7 (Fig. 6). Also, n=1 is assumed in Figs. 5 and 6. For the TE mode [Figs. 5(a) and 6(a)], we note that maximum growth occurs for R_0/R_c=0.654 when ℓ=2 and for R_0/R_c=0.815 when ℓ=7. Evidently, when R_0/R_c is varied, the axial energy spread (Δ) does not influence the value of the <u>maximum</u> growth rate for the TE mode. On the other hand, for the TM mode [Figs. 5(b) and 6(b)], the value of R_0/R_c corresponding to maximum growth depends on the axial energy spread. Moreover, the maximum growth rate for the TM mode is considerably reduced by increasing the axial energy spread. We therefore conclude that the TE mode is a more effective means for exciting radiation with a narrow power spectrum [see

the discussion following Eq. (18)]. In this regard, it is also necessary to select pertrubations with small but nonzero axial wavenumbers, in order for the readiation energy to propagate axially out of the system.

For R_0/R_c=0.633, which corresponds to kR_0=0.5 for the TE mode with $(\ell,n)=(2,1)$, we find numerically that an axial energy spread with $\Delta = 0.3$ is sufficient to stabilize the instability for all harmonic perturbations except $(\ell,n)=(2,1)$. For the present configuration, the next most difficult perturbation to suppress corresponds to $(\ell,n)=(3,1)$. Therefore, exciting microwave radiation with two frequencies, $2\omega_c$ and $3\omega_c$, substantially reduces the axial energy spread required to quench the instability for all harmonic modes except $\ell=2$ and $\ell=3$. It should also be noted from Figs. 5 and 6 that the stabilization produced by the axial energy spread is more effective for high-harmonic perturbations than for low harmonics. This feature is also evident from Eqs. (17) and (22).

Finally, it should be pointed out that the present scheme for producing microwave radiation with a narrow power spectrum (by selecting the value of R_0/R_c close to $\ell/\alpha_{\ell n}$, and by keeping a reasonable amount of axial energy spread) may be most effective for low-harmonic perturbations, since high-harmonic perturbations can be stabilized by a rather small amount of azimuthal energy spread[11].

V. CONCLUSIONS

In this paper, we have examined the excitation of electromagnetic waveguide modes by the negative-mass instability in a relativistic E-layer. The analysis was carried out for an infinitely long E-layer aligned parallel to a uniform magnetic field, within the context of the assumptions that the E-layer is very tenuous [Eq. (1)] and that the electron motion is ultrarelativistic ($\gamma_0 >> 1$). A brief description of the theoretical model and the equilibrium configuration was given in Sec. II. Detailed analytic and numerical results were presented in Secs. III and IV, where the negative-mass stability properties for the TE and TM waveguide modes were investigated for a broad range of system parameters. One of the important conclusions of this study is that the axial energy spread (Δ) has a very important influence on the negative-mass stability behavior for both the TE and TM waveguide modes. Moreover, in the special limiting case when $\Delta=0$, the stability properties for TE mode are consistent with the results previously obtained by Sprangle[14].

Finally, we emphasize that the stability criterion in Eq. (17) suggests a method for controlling the frequency of the TE mode microwave radiation generated by the negative-mass instability. In particular, for perturbations with sufficiently large axial wavenumber ($k \gtrsim 1/R_0$), we conclude that selecting the value of R_0/R_c close to $\ell/\alpha_{\ell n}$, and introducing a modest axial energy spread ($\Delta \gtrsim 1$) can effectively stabilize all modes except (ℓ,n). Moreover, this is more effective for the TE mode than for the TM mode (Secs. III and IV).

ACKNOWLEDGMENTS

This research was supported by the National Science Foundation. The research by one of the authors (H. U.) was supported in part by the Office of Naval Research under the auspices of the University of Maryland-Naval Research Laboratory Joint Program in Plasma Physics.

REFERENCES

1. H. A. Davis, R. A. Meger and H. H. Fleischmann, Phys. Rev. Lett. 37, 542 (1976).
2. M. Friedman, Appl. Phys. Lett. 26, 366 (1975).
3. G. Bekefi and T. Orzechowck, Phys. Rev. Lett. 37, 379 (1976).
4. M. Friedman and M. Herndon, Phys. Fluids 16, 1982 (1973).
5. V. L. Granatstein, P. Sprangle, R. K. Parker, J. Pasour, M. Herndon and S. P. Schlesinger, Phys. Rev. A14, 1194 (1976).
6. V. L. Granatstein, R. K. Parker, and P. Sprangle, Proc. Int. Topical Conf. on Electron Beam Research and Technology, Vol. II, 401 (Albuquerque, New Mexico, 1975).
7. C. H. Dustmann, W. Heinz, H. Krauth, L. Steinbock and W. Zernial, Proc. IXth Int. Conf. on High Energy Accelerators, 250 (Stanford, Calif., 1974).
8. J. Fink, W. Herrmann, W. Ott and J. M. Peterson, Proc. IXth Int. Conf. on High Energy Accelerators, 223 (Stanford, Calif., 1974).
9. W. W. Dastler, D. W. Hudgings, M. J. Rhee, S. Kawasaki and V. L. Granatstein, J. Appl. Phys. in press (1977).
10. Y. Y. Lau and R. J. Briggs, Phys. Fluids 14, 967 (1971).
11. H. Uhm and R. C. Davidson, Phys. Fluids 20, 771 (1977).
12. H. Uhm and R. C. Davidson, "Influence of Axial Energy Spread on the Negative-Mass Instability in a Relativistic Nonneutral E-layer", submitted for publication (1977).
13. R. J. Briggs and V. K. Neil, Plasma Phys. 9, 209 (1967).
14. P. Sprangle, J. Appl. Phys. 47, 2935 (1976).

FIGURE CAPTIONS

Fig. 1 Equilibrium configuration and coordinate system.

Fig. 2 Plots of normalized growth rate ω_i/ω_g versus R_0/R_c obtained from: (a) Eq. (14) (TE mode), and (b) Eq. (20) (TM mode), for Δ=0, n=1 and several values of ℓ.

Fig. 3 Plots of ω_i/ω_g versus R_0/R_c obtained from: (a) Eq. (14) (TE mode), and (b) Eq. (20) (TM mode), for Δ=0, ℓ=8 and several values of n.

Fig. 4 Plots of ω_i/ω_g versus $\Delta=(\Delta E/\gamma_0 mc^2)(\gamma_0/\nu)^{2/3}$ obtained from Eqs. (14) and (20) for ℓ=6, n=1 and normalized axial wave-number kR_0=2.

Fig. 5 Plots of ω_i/ω_g versus R_0/R_c obtained from: (a) Eq. (14) (TE mode), and (b) Eq. (20) (TM mode), for ℓ=2, n=1 and several values of Δ.

Fig. 6 Plots of ω_i/ω_g versus R_0/R_c obtained from: (a) Eq. (14) (TE mode), and (b) Eq. (20) (TM mode), for ℓ=7, n=1 and several values of Δ.

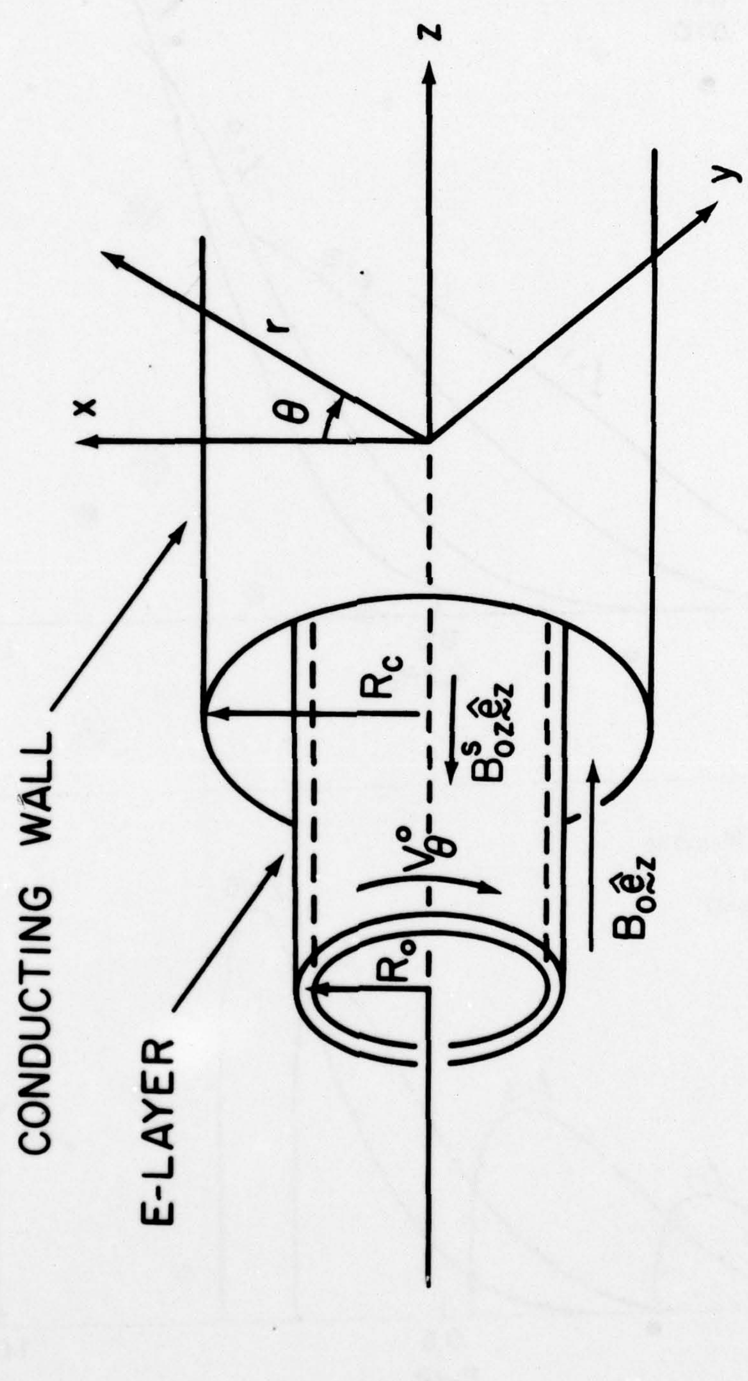
CONDUCTING WALL
E-LAYER
x
z
y
r
θ
R_c
R_o
V_θ^o
$B^s_{oz}\hat{e}_z$
$B_o\hat{e}_z$

Fig. 1

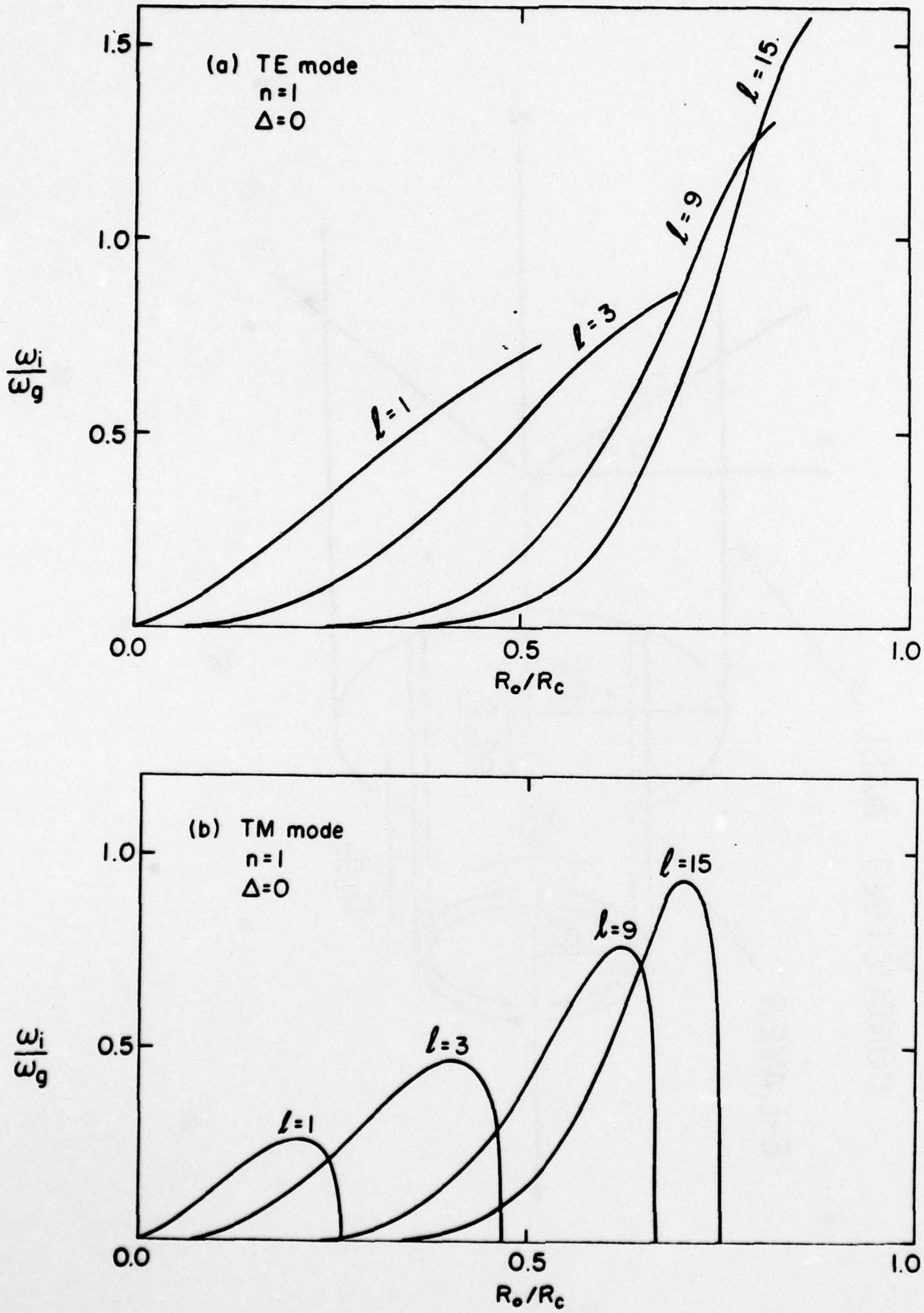

(a) TE mode
n=1
Δ=0
ℓ=1
ℓ=3
ℓ=9
ℓ=15
1.5
1.0
0.5
0.0
0.5
1.0
$\frac{\omega_i}{\omega_g}$
R_o/R_c
(b) TM mode
n=1
Δ=0
ℓ=1
ℓ=3
ℓ=9
ℓ=15
1.0
0.5
0.0
0.5
1.0
$\frac{\omega_i}{\omega_g}$
R_o/R_c

Fig. 2

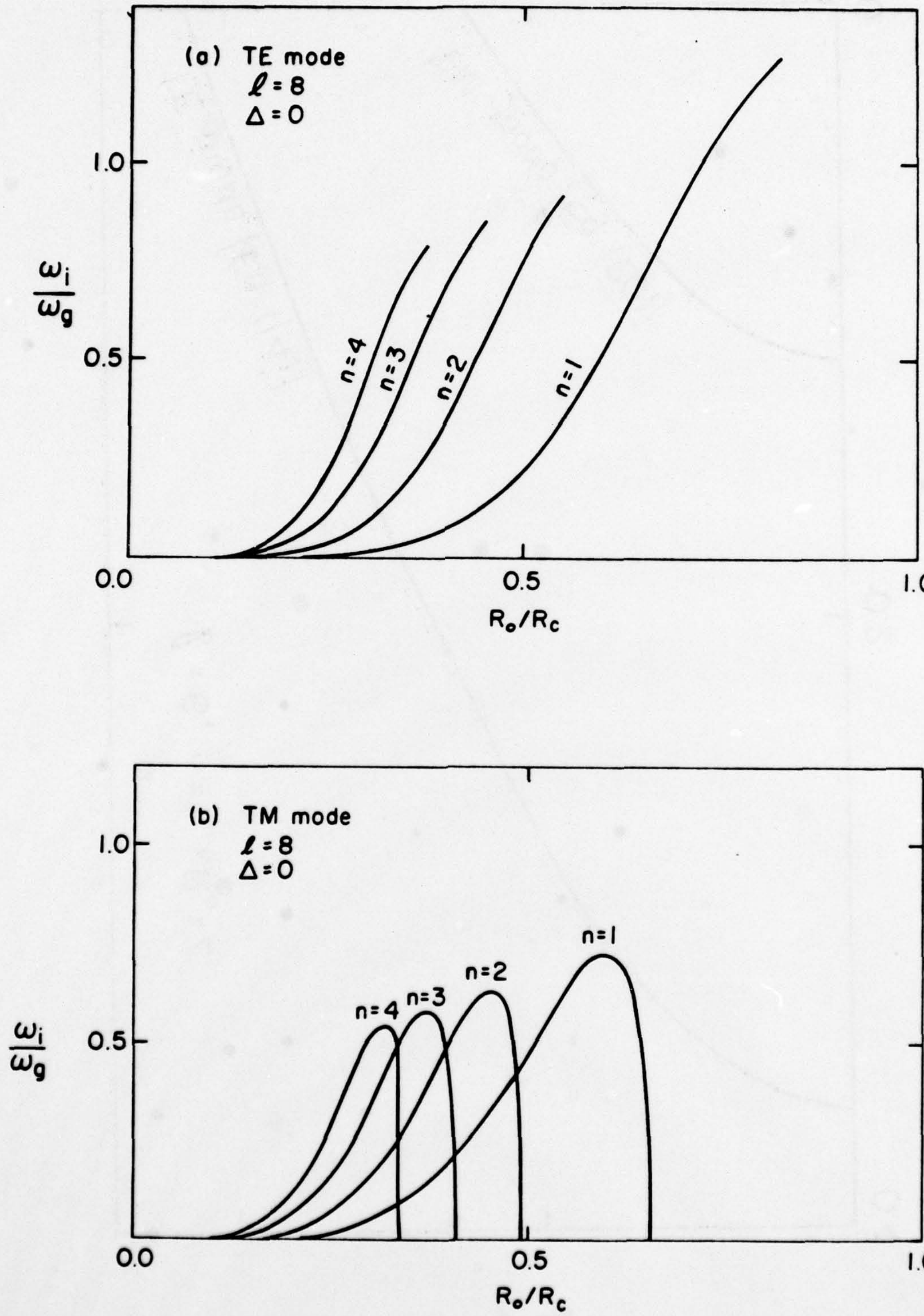

(a) TE mode
ℓ = 8
Δ = 0
1.0
0.5
0.0
1.0
$\frac{\omega_i}{\omega_g}$
n=4
n=3
n=2
n=1
R_o/R_c
(b) TM mode
ℓ = 8
Δ = 0
n=1
n=2
n=3
n=4

Fig. 3

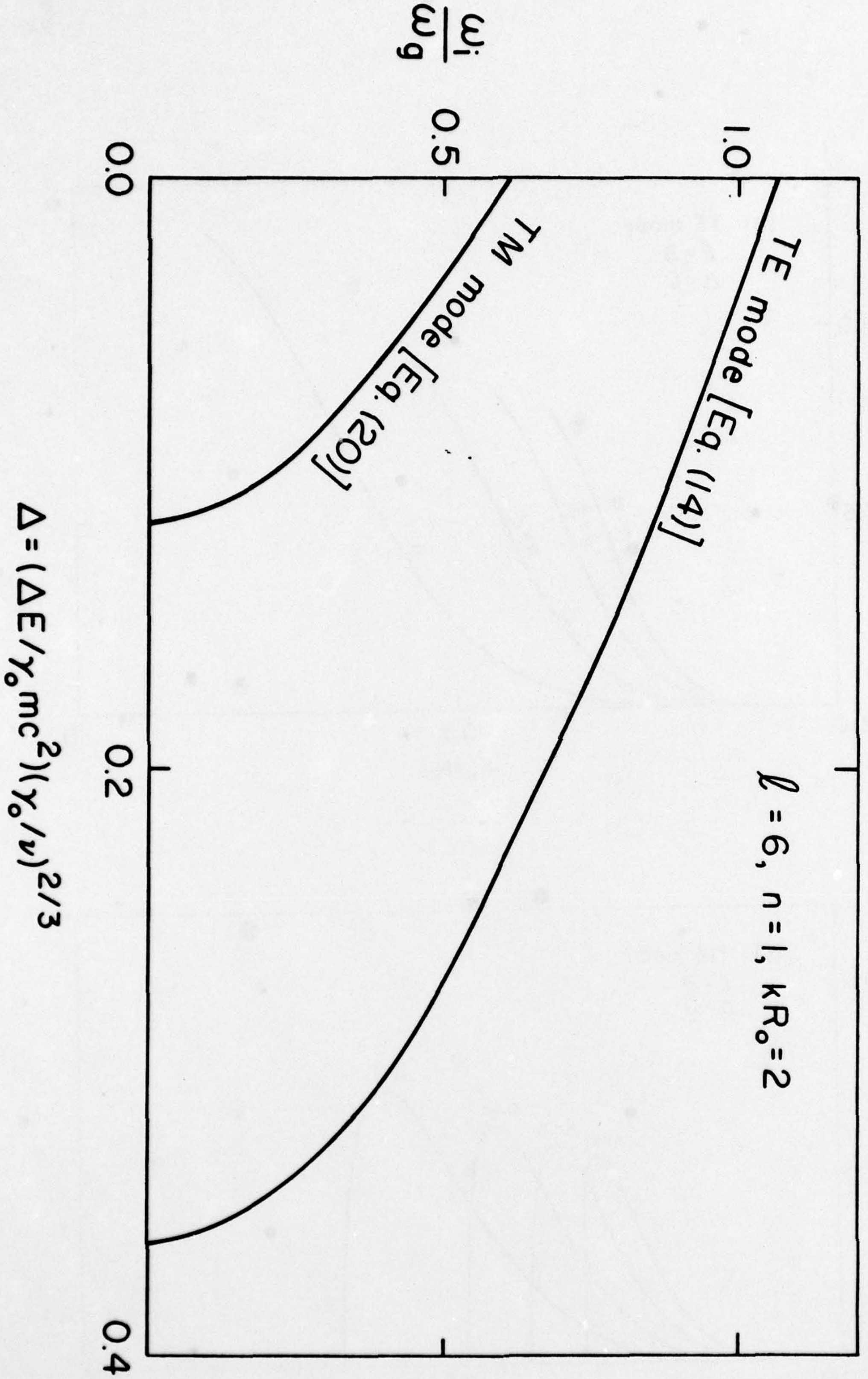

ωi/ωg
0.0
0.5
1.0
0.2
0.4
TE mode [Eq. (14)]
TM mode [Eq. (20)]
ℓ = 6, n = 1, kRo = 2
Δ = (ΔE/γo mc²)(γo/ν)^2/3

Fig. 4

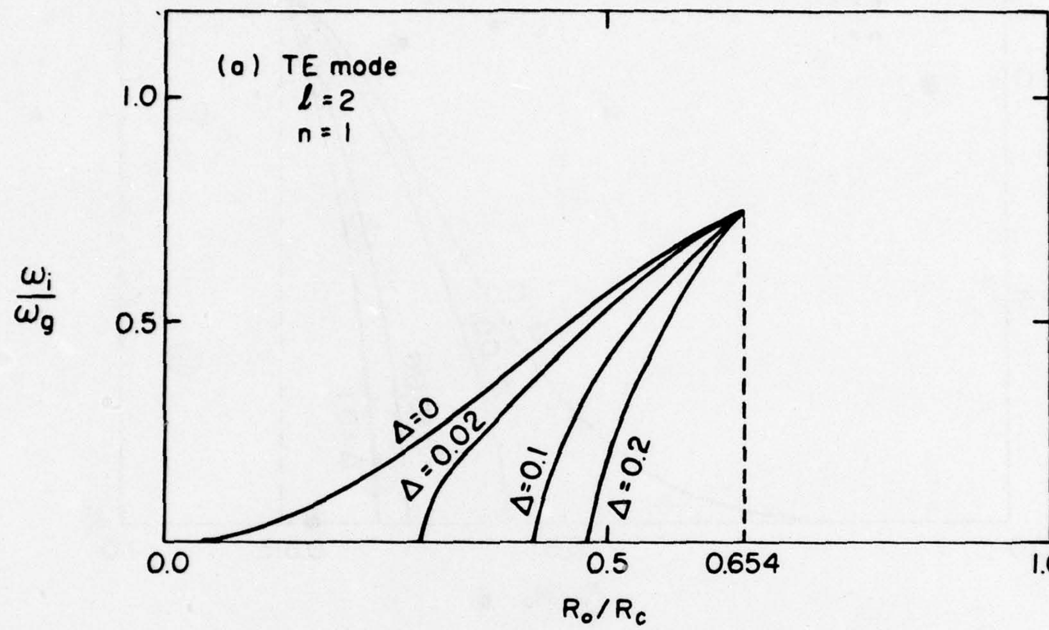
(a) TE mode
$\ell = 2$
n = 1
1.0
0.5
$\frac{\omega_i}{\omega_g}$
Δ=0
Δ=0.02
Δ=0.1
Δ=0.2
0.0
0.5
0.654
1.0
R_o/R_c

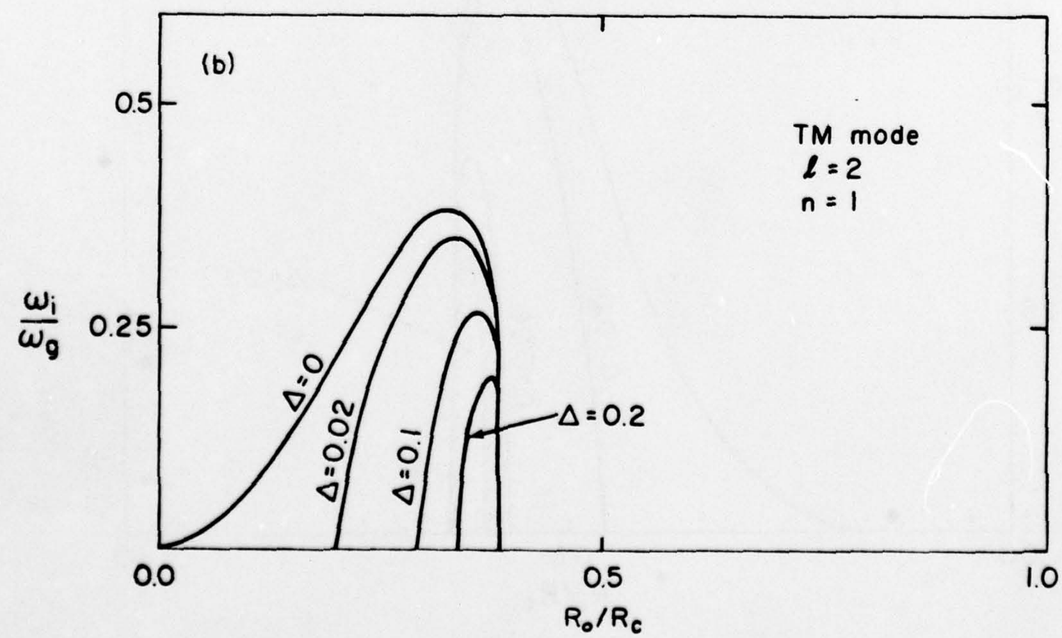
(b)
0.5
0.25
$\frac{\omega_i}{\omega_g}$
TM mode
$\ell = 2$
n = 1
Δ=0
Δ=0.02
Δ=0.1
Δ=0.2
0.0
0.5
1.0
R_o/R_c

Fig. 5

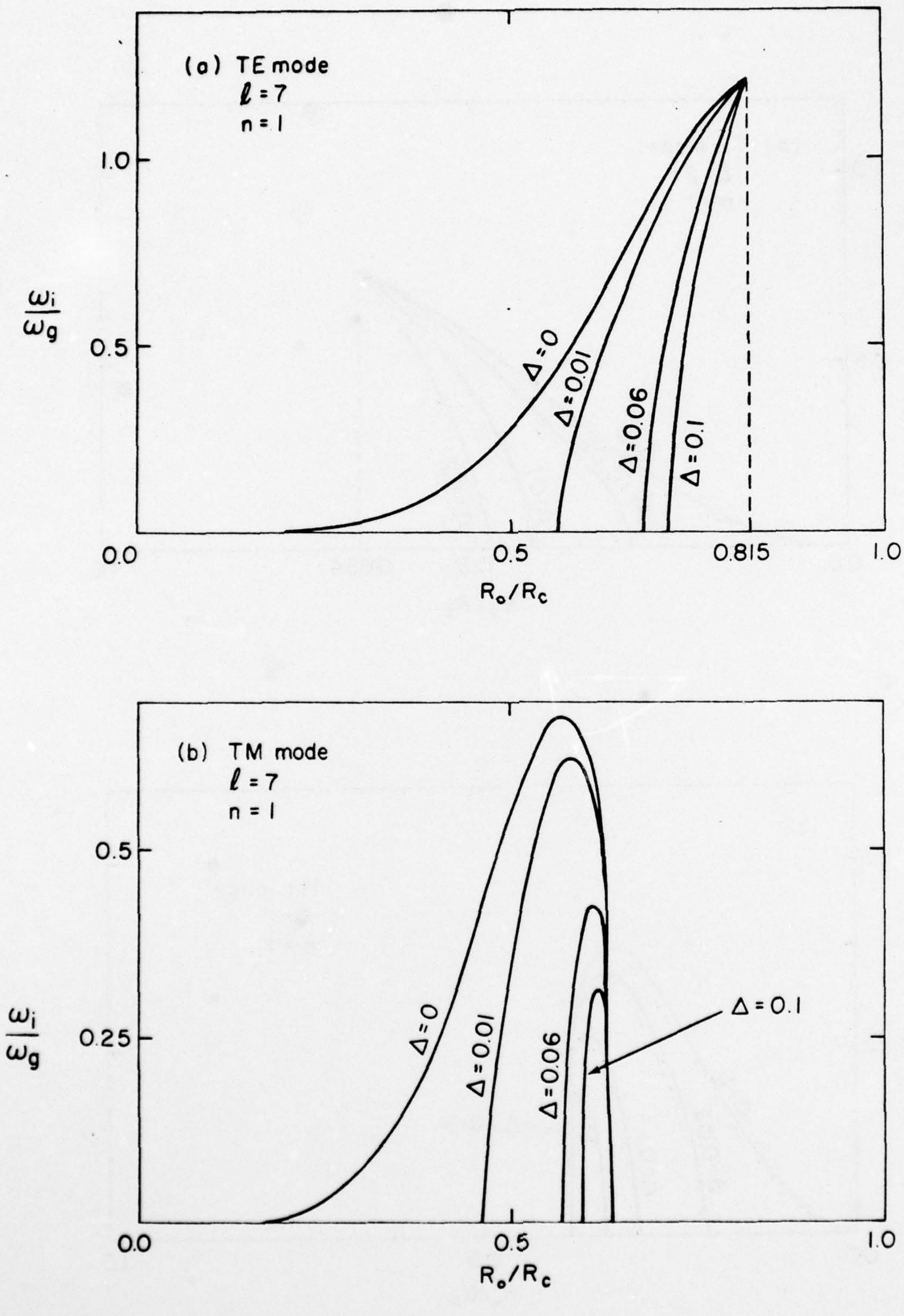
(a) TE mode
ℓ = 7
n = 1
1.0
0.5
$\frac{\omega_i}{\omega_g}$
Δ=0
Δ=0.01
Δ=0.06
Δ=0.1
0.0
0.5
0.815
1.0
R_o/R_c
(b) TM mode
ℓ = 7
n = 1
0.5
0.25
$\frac{\omega_i}{\omega_g}$
Δ=0
Δ=0.01
Δ=0.06
Δ = 0.1
0.0
0.5
1.0
R_o/R_c

Fig. 6